

Naval Research Laboratory

Washington, DC 20375-5000



NRL Memorandum Report 6579

Scaling Z-Pinch Plasmas With Atomic Number for a Given K-Shell Emission

K.G. WHITNEY, J.P. APRUZESE, J.W. THORNHILL AND J. DAVIS

*Radiation Hydrodynamics Branch
Plasma Physics Division*

November 17, 1989

AD-A215 703

This research was sponsored by the Defense Nuclear Agency under Project Task Code and Title, RL RA/Advanced Technology Development, Work Unit Code and Title, 00079, Advanced Technology Development, MIPR No. 89-565.



Approved for public release; distribution unlimited.

89 12 10

SECURITY CLASSIFICATION OF THIS PAGE

REPORT DOCUMENTATION PAGE				Form Approved GMB No. 2704-1188	
1a. REPORT SECURITY CLASSIFICATION UNCLASSIFIED			1b. RESTRICTIVE MARKINGS		
2a. SECURITY CLASSIFICATION AUTHORITY			3. DISTRIBUTION AVAILABILITY OF REPORT Approved for public release; distribution unlimited.		
2b. DECLASSIFICATION/DOWNGRADING SCHEDULE			5. MONITORING ORGANIZATION REPORT NUMBER		
4. PERFORMING ORGANIZATION REPORT NUMBER(S) NRL Memorandum Report 6579			6a. NAME OF PERFORMING ORGANIZATION Naval Research Laboratory		
6b. ADDRESS (City, State, and ZIP Code) Washington, DC 20375-5000			7a. NAME OF MONITORING ORGANIZATION		
8a. NAME OF FUNDING/SPONSORING ORGANIZATION Defense Nuclear Agency			8b. OFFICE SYMBOL (if applicable) RAEV		
8c. ADDRESS (City, State, and ZIP Code) Alexandria, VA 22310			9. PROCUREMENT INSTRUMENT IDENTIFICATION NUMBER		
10. SOURCE OF FUNDING NUMBERS PROGRAM ELEMENT NO 62715N			PROJECT NO TASK NO WORK UNIT ACCESSION NO DN880-191		
11. TITLE (Include Security Classification) Scaling Z-Pinch Plasmas With Atomic Number for a Given K-Shell Emission					
12. PERSONAL AUTHOR(S) Whitney, K.G., Apruzese, J.P., Thornhill, J.W. and Davis, J.					
13a. TYPE OF REPORT Interim		13b. TIME COVERED FROM _____ TO _____		14. DATE OF REPORT (Year Month Day) 1989 November 17	
15. PAGE COUNT 35					
16. SUPPLEMENTARY NOTATION This research was sponsored by the Defense Nuclear Agency under Project Task Code and Title, RL RA/Advanced Technology Development, Work Unit Code and Title, 00079, Advanced Technology Development, MTPR No. 39-363.					
17. COSATI CODES FIELD GROUP SUB-GROUP			18. SUBJECT TERMS (Continue on reverse if necessary and identify by block number)		
			Z-pinch Plasmas		
			Emission X-radiation		
19. ABSTRACT (Continue on reverse if necessary and identify by block number) Simple scaling arguments are developed to show how specification of a desired total K-shell emission can be used to determine the parameters of an imploding array z-pinch plasma as a function of the atomic number of the pinch. The model we use ignores all hydrodynamic details of the z-pinch implosion and thermalization processes and assumes that all of the plasma mass is imploded and thermalized. The pinch is also assumed to be driven by a prescribed linearly rising current. The scaling laws that are derived from these assumptions, in effect, contain phenomenological scaling parameters whose values will need to be more accurately determined by more detailed theoretical calculations and/or by z-pinch experiments on a variety of different machines. (ED)					
20. DISTRIBUTION/AVAILABILITY OF ABSTRACT <input checked="" type="checkbox"/> UNCLASSIFIED/UNLIMITED <input type="checkbox"/> SAME AS RPT <input type="checkbox"/> DTIC USERS			21. ABSTRACT SECURITY CLASSIFICATION UNCLASSIFIED		
22a. NAME OF RESPONSIBLE INDIVIDUAL Dr. Kenneth Whitney			22b. TELEPHONE (include Area Code) (202) 767-2921		
			Code 4720		

DD Form 1473, JUN 86

Previous editions are obsolete

S/N 0102-LF-014-0003

CONTENTS

I.	INTRODUCTION	1
II.	MODEL	1
III.	SCALING ARGUMENTS	4
IV.	RESULTS	8
V.	DISCUSSION AND CONCLUSIONS	13
VI.	ACKNOWLEDGEMENTS	14
VII.	REFERENCES	15
	DISTRIBUTION LIST	27

Accession For		
NTIS GRA&I	<input checked="" type="checkbox"/>	
DTIC TAB	<input type="checkbox"/>	
Unannounced	<input type="checkbox"/>	
Justification		
By _____		
Distribution/		
Availability Codes		
Dist	Avail and/or Special	
A-1		



SCALING Z-PINCH PLASMAS WITH ATOMIC NUMBER FOR A GIVEN K-SHELL EMISSION

I. INTRODUCTION

A major goal in utilizing z-pinch plasmas as high brightness laboratory sources of x-rays for such diverse applications as x-ray lithography, x-ray lasers, materials studies, and plasma spectroscopy is to increase the radiation emission above about 1 keV through the use of moderate atomic number ($Z = 10$ to 36) materials. Two kinds of configuration, single wires and wire arrays or foils¹⁻⁸, have been investigated in the past. Gas puffs can also be used in either geometry though only crudely since the supersonic gas flow at best approximates these shapes. In both cases, it has been observed that optimal x-ray emission decreases on a given machine as the atomic number of the z-pinch material is increased^{2,9}.

Single wire dynamics consists of a complicated interplay between electrical, MHD, ionization, and radiation phenomena. The question, therefore, of how the x-ray emission of these materials will scale with atomic number is, in principle, a difficult one. Wire arrays, on the other hand, initially have a comparatively simple dynamics (to zeroth approximation). A large fraction of the electrical energy is first converted into the kinetic energy of implosion, which is then thermalized when the array collides with itself at the axis of the pinch. In this case, a force and a circuit equation suffice to describe the optimal electrical coupling of the z-pinch load to the pulse power machine¹⁰. In this paper, we will describe how the model of Ref. 10 can be modified and extended to provide predictions of how machine and diode designs must be scaled in order to maintain a given K-shell x-ray emission as the plasma atomic number increases in z-pinch array implosions.

II. THE MODEL

Let m denote the mass per unit length of the wire array or foil and let $r(t)$ be the outside radius of the circular array as a function of time. In response to the magnetic forces that are generated when a current $I(t)$ flows through the array, it accelerates inward:

Manuscript approved April 26, 1989.

$$m \frac{d^2 r}{dt^2} = \frac{1}{2} \frac{\partial L'}{\partial r} I^2 \quad (1)$$

where L' is the array load inductance per unit length¹⁰. For an array consisting of N wires

$$\frac{\partial L'}{\partial r} = - \frac{N-1}{N} \frac{\mu_0}{2\pi} \frac{1}{r} \quad (2)$$

Following Ref. 10, we will utilize the dimensionless variables,

$$x = r/r_0, \quad \tau = t/t_0, \quad i = I/I_0, \quad (3)$$

where r_0 is the initial array radius and

$$t_0 = \frac{N-1}{N} \frac{\mu_0 \ell}{2\pi R_0} = \frac{L_0}{R_0} \quad (4)$$

I_0 is the maximum current that flows in the load, ℓ is the length of the array load, R_0 is the diode resistance, and $L_0 = \mu_0 \ell / (2\pi)$. In terms of these variables, Eq. (1) becomes

$$\frac{d^2 x}{d\tau^2} = - A \frac{i^2}{x} \quad (5)$$

where, for large N , the dimensionless constant A is given by

$$A = \frac{\frac{1}{2}(L_0/\ell)I_0^2}{m(r_0/t_0)^2} \quad (6)$$

For a wide variety of existing pulse power machines, the current pulse is adequately described by a linear ramp $I(t) = \dot{I}_0 t$ during the main run-in phase of the array implosion. In pulse power machines that are designed as current sources, this should also be a useful description of the current pulse. From Eq. (6), one can derive an equation for the increase of kinetic energy with implosion distance:

$$\frac{1}{2} \left(\frac{dx}{d\tau} \right)^2 = A \int_x^1 \frac{i'^2}{x} dx' . \quad (7)$$

It is clear from Eq. (7) that maximum kinetic energy is generated in the implosion if the current is large in the final stages of the run-in. Thus, on both experimental and theoretical grounds, it is useful to investigate the scaling of z-pinch implosions for linearly rising current pulses. For this case, one can define a new dimensionless quantity q by

$$q = q_0 \tau , \quad (8)$$

where

$$q_0 = A^{1/4} (\bar{I}_0 t_0 / I_0)^{1/2} , \quad (9)$$

so that Eq. (5) simplifies to¹¹

$$x \frac{d^2 x}{dq^2} = - q^2 . \quad (10)$$

The picture of array implosions that is provided by Eq. (10) eventually breaks down when the plasma begins to collide on itself and to thermalize the kinetic energy generated prior to this collision. Experimental evidence¹⁰ on implosion times obtained from a number of machines suggests, in fact, that Eq. (10) is generally valid until the plasma has collapsed to about 10% of its initial radius, at which time further collapse is no longer discernible and the main radiation pulse commences. Thus, we will be interested in the solution to Eq. (10) up to values of $x \sim 0.1$ subject to the boundary conditions that the implosion begins at rest $dx/d\tau = 0$ when $x = 1$.

Eq. (10) can be solved either analytically by power series or numerically. The solution information of interest is the final values of q and $(dx/dq)_f$, q_f and $(dx/dq)_f$ respectively, that are achieved when x reaches its final value x_f just prior to the thermalization process. These quantities, obtained from numerical solutions to Eq. (10), are shown in Figures 1 and 2. Least squares fits to the computed values of q_f and $(dx/dq)_f$ are also drawn in these figures. These fits are given by the

polynomial expressions,

$$q_f = 1.73 - 0.22 x_f - 0.42 x_f^2, \quad (11)$$

$$(dx/dq)_f = 4.72 - 18.9 x_f + 49.1 x_f^2, \quad (12)$$

valid for $0.04 \leq x_f \leq 0.14$.

III. Scaling Arguments

By assuming a linear rise in current, one guarantees that the time of array implosion t_f will coincide with the time of peak current. What we would like to require, in addition, is that during the implosion, the array acquires enough kinetic energy to ignite the K-shell and contains enough mass to produce the K-shell emission rates that are required of a high yield super-kilovolt x-ray source. In the process, we would like to determine how these requirements scale with atomic number, Z , from $Z = 10$ (neon) to $Z = 36$ (krypton).

To begin, consider a uniform plasma cylinder of unit length and radius r_f containing a single element of atomic number Z . The amount of mass m contained within this cylinder is

$$m = A m_p N_i \pi r_f^2, \quad (13)$$

where A is the atomic weight of the element, m_p is the mass of a proton, and N_i is the ion density of the plasma. A least squares polynomial fit to $\log A$ as a function of Z results in

$$A \approx 1.58 Z^{1.1}. \quad (14)$$

This functional fit, up to $Z = 36$, to the atomic weights is shown in Figure 3. Thus

$$m(\mu\text{g/cm}) = 8.28 \times 10^{-18} N_i^2 r_f^2 Z^{1.1} \quad (15)$$

In this paper, we will employ a mixed set of MKS units that are appropriate to a discussion of z-pinch. Thus, we will generally express distances and ion densities in units of centimeters and cm^{-3} , masses in units of

micrograms, yields in kilojoules, energies and temperatures in eV, currents in mega-amperes, and time in nanoseconds or microseconds.

There are two ways to determine the scaling of K-shell yield with atomic number. One is by a simple theoretical argument, the other is by an analysis of previous and future experimental and theoretical data. Because of its large oscillator strength, the He- α $1s^2$ - $1s2p$ line dominates the K-shell emission from low density, optically thin plasmas. Thus, one can argue on the basis of the optically thin emission rate of this line that the yield per unit length, y , of total K-shell emission will scale as a power of N_i and inversely as a power of Z . The coefficient of proportionality C_y can be determined either from direct spectroscopic measurements of N_i and T_e made in previous low atomic number z-pinch shots for which an optimal K-shell yield was approximately obtained or from theoretical calculations. One then finds that

$$y(\text{kJ/cm}) \approx C_y N_i^\alpha Z^{-\beta} E(Z) r_f^\gamma \quad (16)$$

where $E(Z)$ is an exponential function of Z to be defined shortly.

Estimates for the exponents, α , β , and γ can be obtained from the following coronal equilibrium arguments. As the atomic number of a given sized plasma is increased, the photon probabilities of escape in the resonance lines of helium or hydrogen approach 1. Thus, the K-shell radiation rates of the plasma become increasingly optically thin. In this case, the amount of He- α emission from our uniform plasma cylinder of unit length will be

$$y_{\text{He-}\alpha} = N_{\text{He}} N_e X_{1s-2p} \Delta E \pi r_f^2 \tau_K \quad (17)$$

where N_{He} is the number of ions in the helium-like ground state, N_e is the electron density, X_{1s-2p} is the rate coefficient for exciting the $1s2p^1P$ state from the ground state, ΔE is the energy of the transition and of the radiated photon, and τ_K is the duration of the emission. To determine the scaling of $y_{\text{He-}\alpha}$ with N_i and Z we use Seaton's formula for the collisional excitation rate for dipole allowed transitions¹²:

$$X_{1s-2p}(\text{cm}^3/\text{sec}) = 1.6 \times 10^{-5} f g \frac{e^{-\Delta E/T_e}}{\Delta E T_e^{1/2}}, \quad (18)$$

where f is the oscillator strength, g is the thermally averaged gaunt factor ~ 1 , and T_e is in units of eV. The temperature T_e for which K-shell occupation and excitation is strong does not scale, as ΔE does, with Z^2 because of the different Z dependences of the collisional ionization and radiation recombination rates. Based on estimates of ionization equilibrium in hydrogen, we will take this scaling to be

$$T_e(\text{eV}) \approx 0.3 Z^{2.9}, \quad (19)$$

although a more detailed analysis of this scaling should be made. Thus,

$$X_{1s-2p} \sim E(Z) / Z^{3.45}, \quad (20)$$

where, because $\Delta E \sim Z^2$ and $T_e \sim Z^{2.9}$, we take $E(Z) = \exp(-20.6/Z^{0.9})$. In order to determine the scaling of τ_K with Z , we assume that K-shell emission is proportional to the inertial confinement time of the plasma during emission:

$$\tau_K \sim \frac{r_f}{v_{th}} = \frac{r_f}{(2kT_e/A m_p)^{1/2}} \sim r_f / Z^{0.9}. \quad (21)$$

Thus, in coronal approximation,

$$y_{\text{He-}\alpha} \sim \frac{N_i^2 r_f^3 E(Z)}{Z^{1.35}}, \quad (22)$$

and, in this case, taking y and $y_{\text{He-}\alpha}$ to scale identically with Z and N_i we find that $\alpha \approx 2$, $\beta \approx 1.35$, and $\gamma \approx 3$.

If the K-shell of a given element is to be excited, a minimum energy must be imparted to each imploding ion in order to (1) strip all but one or two electrons from the ion and (2) maintain each stripped electron at

temperatures to avoid recombination back into the L-shell. Of course inefficiencies in the thermalization process, in particular subkilovolt radiative losses, imply that much more energy than this is needed in practice. However, an initial insight into basic Z-scaling may be obtained by consideration of these basic quantities.

As noted, the temperatures at which maximum amounts of K-shell radiation are expected are $T_e \approx 0.3 Z^{2.9}$. We approximate the number of stripped electrons as equalling Z. Therefore, the thermal energy of the stripped electrons from an ion of atomic number Z at this temperature is,

$$E_t = 0.4 Z^{3.9} \text{ eV/ion.} \quad (23)$$

The energy needed to strip the electrons from each ion is also important and non-negligible. We shall assume that the plasma is 50% hydrogen-like and 50% helium-like. The ionization potentials for each element are available from many references; we have used the data of Carlson et al.¹³ The energy needed is given by the following fit - which for purposes of the approximate treatment of this paper has negligible error:

$$E_s = 3.83 Z^{2.64} \text{ eV/ion.} \quad (24)$$

Obviously, the minimum energy per ion that must be acquired during thermalization is given by $E_t + E_s$. A critical question is, in practice however, how much energy per ion beyond the minimum is required for optimum K-shell radiation to be generated in a z-pinch? We will assume that the kinetic energy per ion that must be generated in an array implosion is some multiple, ϵ , of this minimum energy. From past analyses of aluminum experimental data, there is some indication that $\epsilon \sim 15$ and that it may be as large as 30. We now make the assumption that, for all Z, ϵ (~ 15) times $(E_t + E_s)$ will be required for efficient K-shell radiation production. Such a large factor is plausible when one considers the numerous sinks for generator energy other than production of K-shell radiation. Such processes include runaway electron production during the implosion, the generation of axial plasma motions, nonuniform thermalization and radiative losses other than K-shell. This is not unreasonable as a first approximation since it allows radiative and other losses to scale upward with Z in the same fashion as the thermal and ionization energies, which is

initially reasonable. Beginning with a factor of 15 can be viewed optimistically, since it indicates that improvements in the efficiency of these devices may be achievable. This assumption means that

$$\begin{aligned} \frac{1}{2} m_i \left(\frac{dr}{dt} \right)_f^2 &= (KE)_{ion} = 1.6 \times 10^{-19} \epsilon (0.4 Z^{3.9} + 3.83 Z^{2.64}) \\ &= 2.39 \times 10^{-19} \epsilon Z^{3.51} \text{ (J/ion)}, \end{aligned} \quad (25)$$

where, in Eq. (25), the additional simplification of the power-law sum to a single power law does not result in substantial error for present purposes.

IV. RESULTS

Equations (11), (12), (14), (15), (16), (19), and (25) allow one to determine the scaling of the mass loading, implosion time, and the rate of current rise, \dot{I}_0 (I-dot), with atomic number in order to achieve a given K-shell yield. For example, on eliminating N_i from Eqs. (15) and (16), one finds that

$$m \text{ (}\mu\text{g/cm)} = C_m y^{1/\alpha_r} (2-3/\alpha) Z^{(1.1+\beta/\alpha)} E(Z)^{-1/\alpha}, \quad (26)$$

where $C_m = 8.28 \times 10^{-18} / C_y^{1/\alpha}$. The implosion time is $t_f = (t_o/q_o) q_f$; it can be found from Eqs (11), (12), and (25) since

$$\left(\frac{dr}{dt} \right)_f = \frac{q_o r_o}{t_o} \left(\frac{dx}{dq} \right)_f = \frac{q_f r_o}{t_f} \left(\frac{dx}{dq} \right)_f. \quad (27)$$

Thus,

$$t_f = q_f \left(\frac{dx}{dq} \right)_f \left(\frac{m_i}{2(KE)_{ion}} \right) r_o, \quad (28)$$

where we now write $(dx/dq)_f$ for the magnitude of this final velocity. Finally, we note that the I-dot of the implosion can be determined from Eqs. (6), (9), (28) and the relationship $t_f/q_f = t_o/q_o$:

$$\frac{t_o}{q_o} = \left(\frac{m r_o^2}{1/2 L_o I_o^2} \right)^{1/4} \frac{t_f}{q_f} = \left(\frac{dx}{dq} \right)_f \left(\frac{m_i}{2(KE)_{ion}} \right)^{1/2} r_o, \quad (29)$$

i.e.,

$$I_o = \left(\frac{4\pi m}{\mu_o} \right)^{1/2} \left\{ \frac{q_f^2 r_o}{t_f^2} \right\} = \left\{ \frac{2(KE)_{ion}}{m_i r_o} \right\} \left(\frac{4\pi m}{\mu_o} \right)^{1/2} \left(\frac{dx}{dq} \right)_f^2. \quad (30)$$

For a given yield and initial array radius, all of the quantities on the right hand sides of Eqs. (26), (28), and (30) are scalable with Z , assuming that conventional wisdom is correct and back EMF's and plasma pressure forces will stop the 1-d implosion and begin to thermalize the kinetic energy at or around a value of $x_f \sim 0.1$ (see Ref. 10). In order to illustrate this procedure in more detail, we will now specialize to two cases where $\alpha=2$, $\beta=1.35$, and $\gamma=3$ (see Eq. 22) and, from experimental estimates, we take C_y to be 9.1×10^{-33} . Eqs. (26), (28), and (30) then become

$$m \text{ (}\mu\text{g/cm)} = 8.68 \times 10^{-2} (yr)_f^{1/2} Z^{1.776} \exp(9.2/Z^{0.9}), \quad (31)$$

$$t_f \text{ (ns)} = 7.5 \times 10^2 q_f (dx/dq)_f r_o Z^{-1.205} \epsilon^{-0.5}, \quad (32)$$

$$I_o \text{ (MA/}\mu\text{s)} = 4.44 \times 10^{-5} (dx/dq)_f^2 \epsilon \frac{(yr_f)^{1/4} Z^{3.3}}{r_o} \exp(4.6/Z^{0.9}), \quad (33)$$

where as mentioned earlier, y is expressed in units of kJ/cm and r_o and r_f in units of cm. Graphs of these scaling relations are shown in Figures 4-6 for two cases.

In case I, we took the initial radius of the array to be 1 cm, and assumed $x_f=0.1$, so that $q_f=1.7$, $(dx/dq)_f=3.3$, and $r_f=0.1$ cm. The desired yield was taken to be 2kJ/cm and the thermalization efficiency, $\epsilon=15$. In

case II, these values were taken to be: $r_o=2$ cm, $x_f=0.07$, $q_f=1.71$, $(dx/dq)_f=3.63$, $r_f=0.14$ cm, $y=15$ kJ/cm, and $\epsilon=10$.

It is clear from Eqs. (31) - (33) and from Figs. 4-6 that array implosions must start at a large radius and implode to a fairly tight cylinder on axis with a good kinetic-to-thermal conversion efficiency in order to produce high K-shell yields with long implosion times and small I-dots. Moreover, for a given machine, with given I-dot and current capabilities, the optimum choice of element depends on the yield-per-length and spectrum requirements. It is also clear, however, that the pulse power machine must be redesigned as the load element or yield requirement is changed.

The above scaling relations derive from the assumptions of an optically thin plasma and an impressed linearly rising current across the plasma that terminates at the time of kinetic energy thermalization. Figure 7, which shows the ion densities that are computed from Eq. (15) and (31), indicates that the first assumption holds up in the two cases under study very well. As to the second assumption, we replaced the voltage source utilized in Katzenstein's work¹⁰ with a current source with obvious fundamental consequences, since array implosions are current driven.

In general, the ohmic resistance of the array plasma is small, so that the voltage drop across the load $V_\ell(t)$ is given by $V_\ell = d(L_\ell I)/dt$, where the load inductance L_ℓ for an N-wire array of wire diameter d_w having a return current path radius R is given by¹⁰:

$$L_\ell = L_o \left(\frac{1}{N} \ln \left(\frac{R}{Nd_w} \right) + \frac{N-1}{N} \ln \left(\frac{R}{r} \right) \right) \quad (34)$$

Hence

$$\frac{dL_\ell}{dt} \approx L_o \frac{1}{r} \left(-\frac{dr}{dt} \right), \quad (35)$$

and

$$V_\ell = \dot{I}_o \left(L_\ell + L_o (t/r)(-dr/dt) \right). \quad (36)$$

After converting to dimensionless variables, one finds that the voltage drop across the load at the end of the implosion, $V_{\ell f}$, is

$$V_{\ell f} = \left(L_{\ell} + (q_f/x_f)(dx/dq)_f L_o \right) \overset{\circ}{I}_o . \quad (37)$$

By virtue of Eq. (33), therefore, it follows that $V_{\ell f}$ scales as $Z^{3.3}$.

In general, the second term in Eq. (37) dominates over the first. As the load collapses, therefore, maintenance of a steadily rising current requires a disproportionately large rise in the voltage across the plasma near the end of the collapse. This point is demonstrated in Figures 8 and 9. We have defined the peak current I_o to be $\overset{\circ}{I}_o t_f$. For an array length of 2 cm, we see from Figures 8 and 9 that peak currents of near 2 MA in aluminum generate peak voltages at the end of the collapse near 7 MV. For selenium, however, peak currents of 11 MA and 14 MA are needed in the two cases and they produce peak voltages near 150 MV. Under these conditions, pulse power machines will not act as current sources and the current will generally take a steep dip at the time of the final collapse of the plasma on axis, rendering the assumption of a linear current rise invalid. For this reason, the scaling relations developed in this paper will generally need some correcting and/or to be empirically determined under experimental conditions that implode the arrays in the required times and give them the required final kinetic energy per ion.

One theoretical feature of the Eqs. (19) - (33) scaling relations, already has some experimental support: that of the scaling of yield with peak current for optimal yields. Since $I_o = \overset{\circ}{I}_o t_f$, it follow from Eq (30) that

$$m(\text{kg/m}) = \frac{\mu_o}{4\pi} \left\{ \frac{t_f}{q_f^2 r_o} \right\}^2 I_o^2 . \quad (38)$$

Therefore, from Eqs. (13) and (16) (with $\alpha=2$, $\beta=1.35$, and $\gamma=3$) one finds that

$$y(\text{kJ/cm}) = 2.6 \times 10^{-16} E(Z) \left\{ \frac{I_o^4}{r_f Z^{8.37}} \right\} . \quad (39)$$

Thus, the scaling relations can be rewritten to exhibit an I^4 scaling of the yield on peak current. In the context of a fixed pulse power machine, such scaling has been observed experimentally for optimal K-shell yields in neon.¹⁴

It is also of interest to determine what the scalings of Eq. (31) - (33) predict on average about the balance of pressure, f_p , and magnetic field, $f_{j \times B}$, forces per unit length at the end of the implosion. Using Eqs. (13) and (19), we find (in MKS units) that

$$\begin{aligned} f_p &\equiv 2\pi r_f p_f \approx 2\pi r_f Z N_i k T_e \\ &= 4.8 \times 10^{-20} (2m/(m_i r_f)) Z^{3.9}. \end{aligned} \quad (40)$$

Also, from Eqs. (25), (28), and (30),

$$\begin{aligned} f_{j \times B} &\equiv \frac{\mu_0 I_0^2}{4\pi r_f} = \\ &= 2.39 \times 10^{-19} \left(\frac{2m}{m_i r_f} \right) \frac{q_f^2}{(dx/dq)_f^2} \epsilon Z^{3.51}. \end{aligned} \quad (41)$$

These forces will be equal only for a particular thermalization efficiency

$$\epsilon = 0.2 \left(dx/dq \right)_f^2 Z^{0.39} / q_f^2, \quad (42)$$

which, in the two cases under consideration in this paper, has the values (<4) displayed in Figure 10. Since ϵ is expected to have values much larger than those in Figure 10, $f_{j \times B}$ will be much larger than f_p . However, as noted above, in reality, the current will dip sharply at the moment the plasma arrives on axis. Thus, the collapse will be stopped as the forces reverse in strength. This accounts, to some extent, for the empirical observation that $x_f \sim 0.1$. Plasma instability development may also contribute to this effect.

V. Discussion and Conclusions

The basic idea underlying the scaling relations of Eqs. (31) - (33) is that if z-pinch x-ray sources with a given yield and successively higher kilovolt energies are to be developed, then one must redesign the pulse power machine as the atomic number of the plasma is increased in order to implode the required higher plasma mass with a higher power input and a shorter implosion time (for a given plasma load geometry). It follows, conversely, that if the machine is not redesigned or reconfigured to the plasma, that one can expect the yield of K-shell x-rays to fall as the atomic number of the plasma is increased in conformity with experimental observations.⁹ It also follows that the theoretical convenience of a linearly rising current pulse should not be strictly required experimentally, provided the required mass can be imploded to the required final kinetic energy by an appropriate circuit design.

The more fundamental scaling relations of this paper are given by Eqs. (26), (28), and (30) with α , β , γ , ϵ , x_f , q_f , and $(dx/dq)_f$ regarded as empirical constants to be determined ultimately, either from experimental data or from 1-d hydrodynamic computer simulations of the array or foil implosion process. Simulations are needed, in particular, in order to determine (1) the thermalization efficiency, ϵ , of foil implosions and (2) whether or not this efficiency itself is a scalable function of Z and/or a function of yield. We carried out some preliminary 1-d calculations for a titanium foil. They suggest that thermalization efficiencies of 15 do occur for a certain class of implosions. One major limitation of these calculations is that they do not describe the instability growth that is known to occur experimentally, and that undoubtedly plays a role in limiting the application of the above theory and the extent of the implosion (i.e. the size of x_f) and, thus, the thermalization efficiency. However, it should also be noted that experiments conducted to date, in which instability growth was observed and in which the implosion was limited, were generally non-optimally designed (as described in this paper) for radiation production in the K-shell. Another factor that may limit the range of validity of these scaling relations is the tendency of z-pinchs to undergo radiative collapse.^{15,16} If the mass loading is sufficiently

high or if instabilities form, the plasma will implode to radii much smaller than $0.1 r_0$.

Finally, important experimental evidence of non-optimum performance is frequently provided by filtered pinhole pictures of the z-pinch emission region.^{2,3} It is generally observed that as the energy of the photons increases, the size of the corresponding emission region decreases. Depending on the pulse power machine, this generally means that as Z increases, the fraction of the foil mass that participates in the K-shell emission decreases. In this sense, Z-pinch plasmas, like vacuum sparks, are remarkably accommodating. When more plasma than can be ionized to the K-shell is imploded, only an appropriate fraction, matched to the power capabilities of the circuit, is heated to produce the K-shell emission. This experimental behavior contrasts with one of the basic assumptions of the model calculations of this paper that all of the foil mass that is accelerated inward participates in the subsequent thermalization and K-shell emission. Any experiments that are conducted to test the scaling relations proposed in this paper should carefully examine the validity of this mass participation assumption.¹⁷

VI. Acknowledgements

This work was supported by the Defense Nuclear Agency and the Office of Naval Research.

References

1. D. Mosher, S. J. Stephanakis, I. M. Vitkovitsky, C. M. Dozier, L. S. Levine, and D. J. Nagel, Appl. Phys. Lett. 23, 429 (1973)
2. P.G. Burkhalter, C. M. Dozier, and D. J. Nagel, Phys. Rev. A 15, 700 (1977).
3. P. G. Burkhalter, J. Davis, J. Rauch, W. Clark, G. Dahlbacka, and R. Schneider, J. appl. Phys. 50, 705 (1979).
4. P. J. Turchi, and W. L. Baker, J. Appl. Phys. 44, 4936 (1973).
5. C. Stallings, C. K. Nielsen, and R. Schneider, Appl. Phys. Lett. 29, 404 (1976).
6. W. Clark, M. Wilkinson, J. Rauch, and J. LePage, J. Appl. Phys. 53, 1426 (1982).
7. W. Clark, M. Gersten, J. Katzenstein, J. Rauch, R. Richardson, and M. Wilkinson, J. Appl. Phys. 53, 4099 (1982).
8. S. M. Zakharov, G. V. Ivanenkov, A. A. Kolomenskii, S. A. Pikuz, and A. I. Samokhin, Fiz. Plazmy 13, 206 (Sov. J. Plasma Phys. 13, 115) (1987).
9. W. Clark, M. Gersten, D. Tanimoto, A. Kolb, J. Pearlman, J. Rauch, R. Richardson, J. Riordan, and M. Wilkinson, "Imploding Plasma Pinches Driven by High Power Generators," in Proceedings of Fifth International Conference on High Power Particle Beams 1983, University of California, San Francisco, California, (1983), p.236-241.
10. J. Katzenstein, J. Appl. Phys. 52, 676 (1981).
11. J. P. Apruzese and J. Davis, "K-shell Yield Scaling Law for Conventional PRS Loads," NRL Memorandum Report 5406 (1984).

12. M. J. Seaton, in "Atomic and Molecular Processes", ed. by D. R. Bates, Academic Press, New York, (1962), p. 374.
13. T. A. Carlson, C. W. Nestor, Jr., N. Wasserman, and J. D. McDowell, Atomic Data 2 63 (1970).
14. S. J. Stephanakis, J. P. Apruzese, P. G. Burkhalter, J. Davis, R. A. Meger, S. W. McDonald, G. Mehlman, P. F. Ottinger, and F. C. Young, Appl. Phys. Lett., 48 (13), 829 (1986).
15. J. W. Shearer, Phys. of Fluids 19, 1426 (1976).
16. V. V. Vikhrev, V. V. Ivanov, and K. N. Koshelev, Fiz. Plazmy 8, 1211 (1982). (Sov. J. Plasma Phys. 8(6), 688 (1982).)
17. M. C. Coulter, and K. G. Whitney, "Procedures for Analyzing Z-pinch X-ray Data," Bull. Amer. Phys. Soc. 33(9), paper 2W9 (1988).

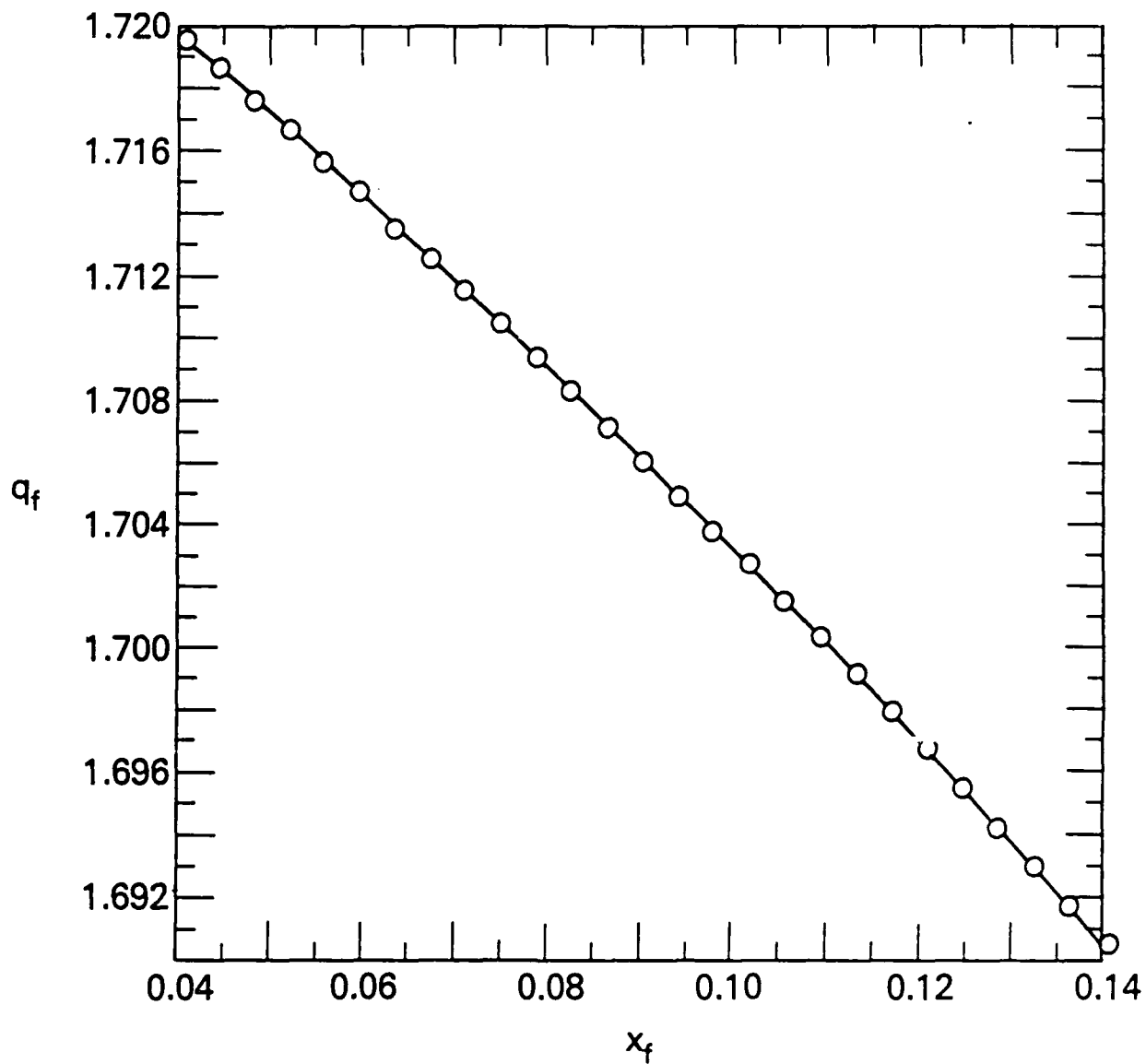


Figure 1. A least squares polynomial fit to calculated values of q_f is shown valid for values of x_f between 0.04 and 0.14.

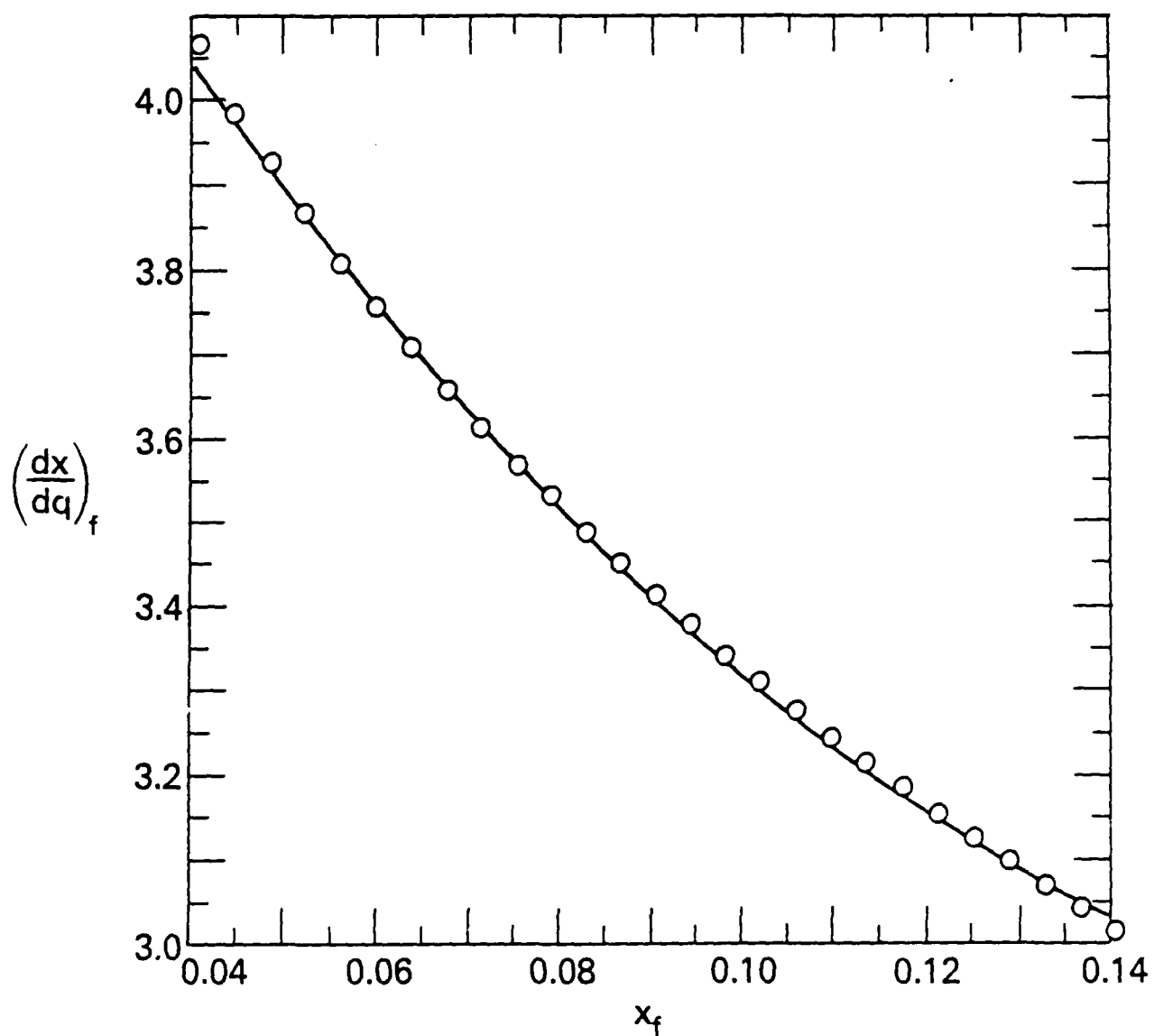


Figure 2. A least squares polynomial fit to calculated values of $(\frac{dx}{dq})_f$ is shown valid for values of x_f between 0.04 and 0.14.

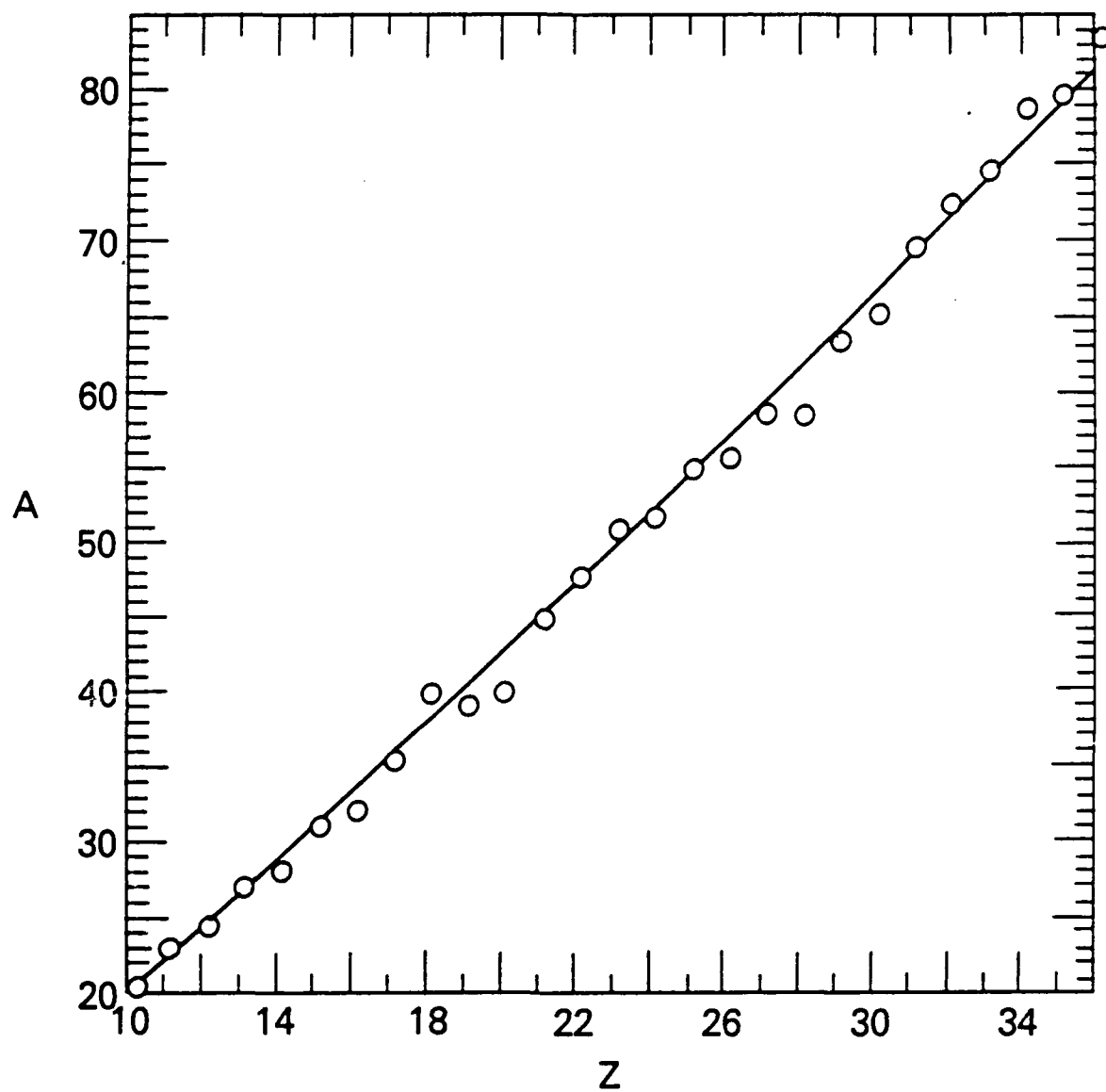


Figure 3. The atomic weights between neon ($Z=10$) and krypton ($Z=36$) are drawn relative to the curve fit $A=1.58Z^{1.1}$.

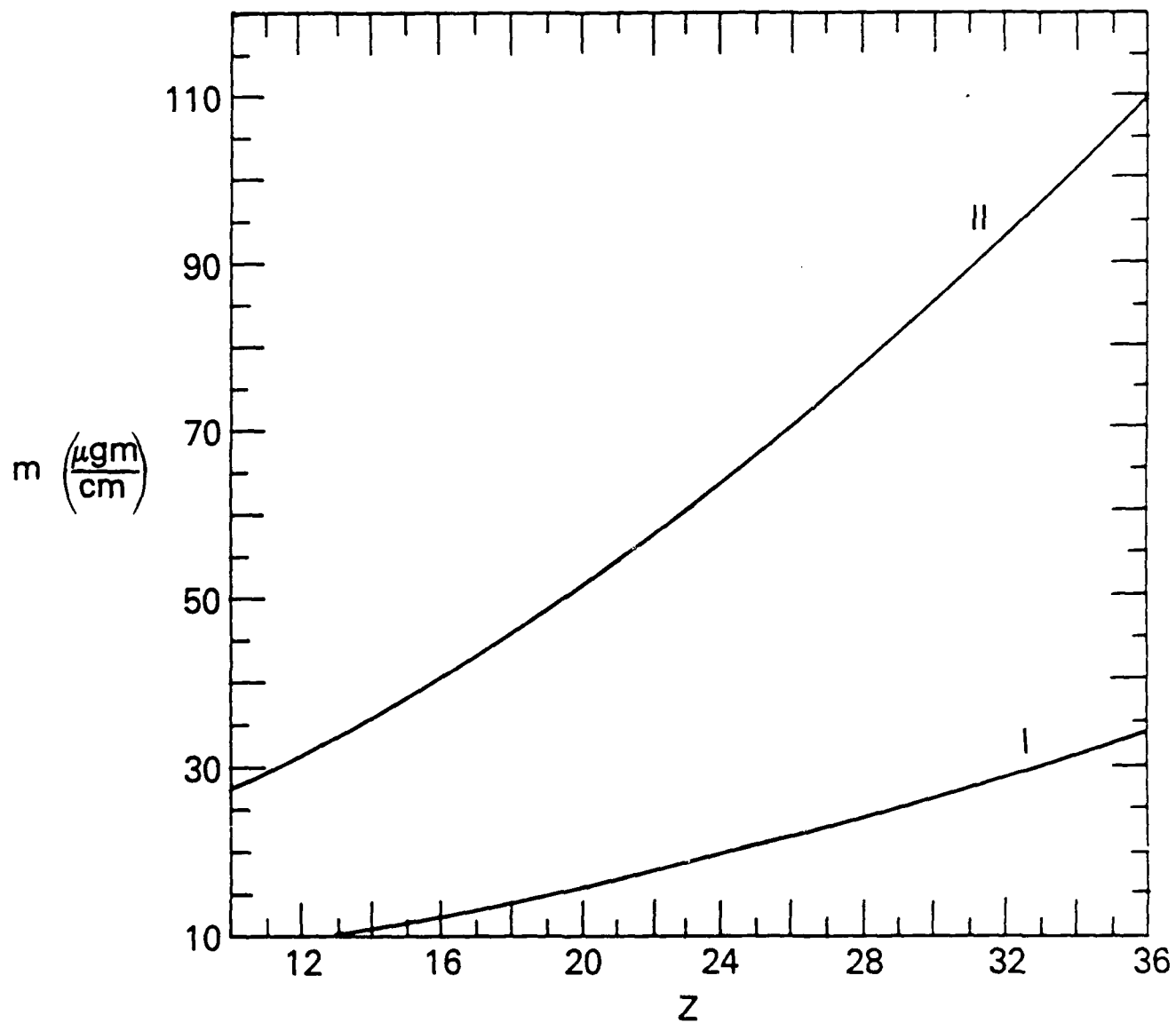


Figure 4. The scaling of the mass-per-length of a z-pinch array as a function of atomic number is shown for the two cases (I and II) described in the text.

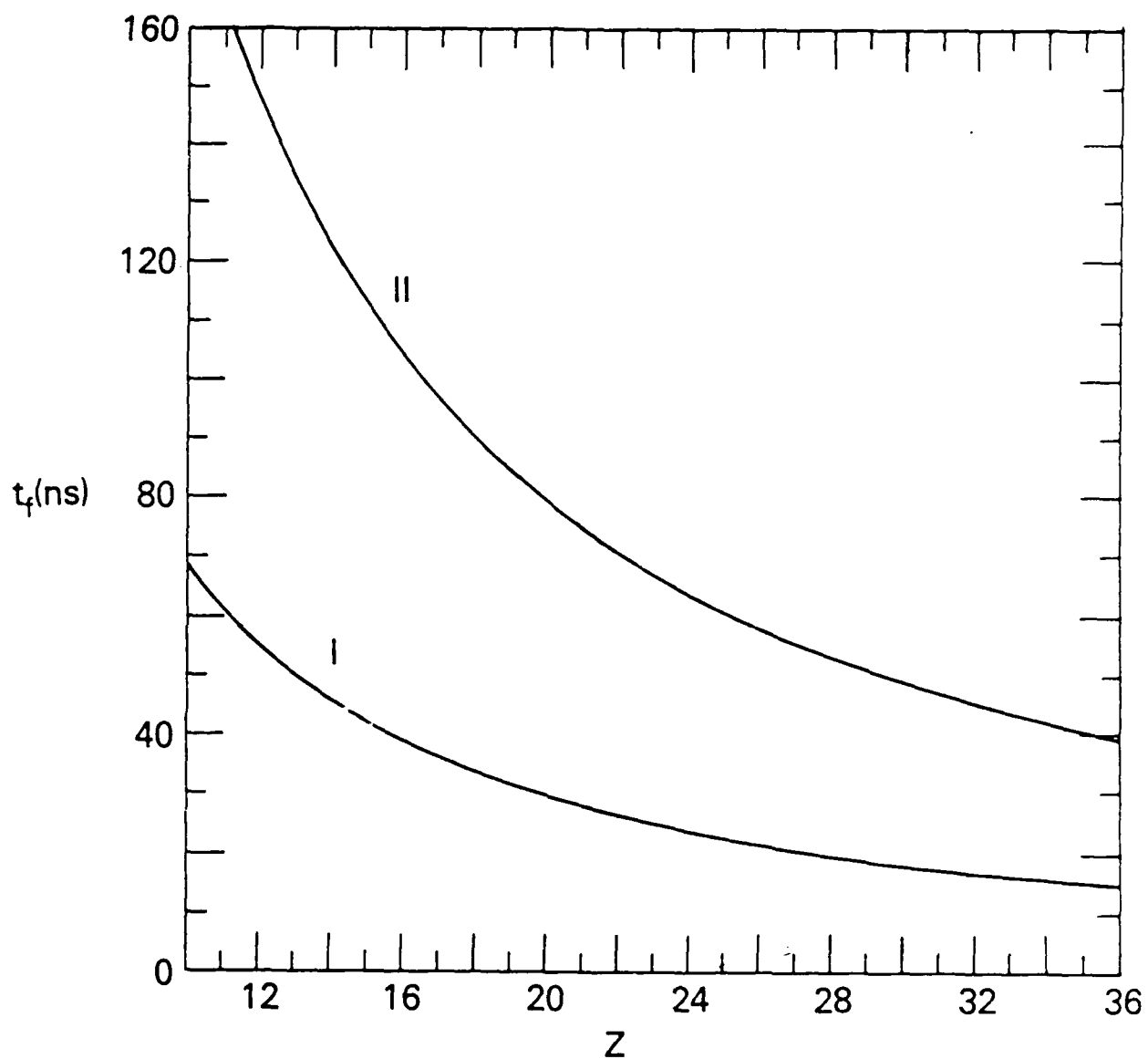


Figure 5. The scaling of the array implosion time as a function of atomic number is shown for the two cases (I and II) described in the text.

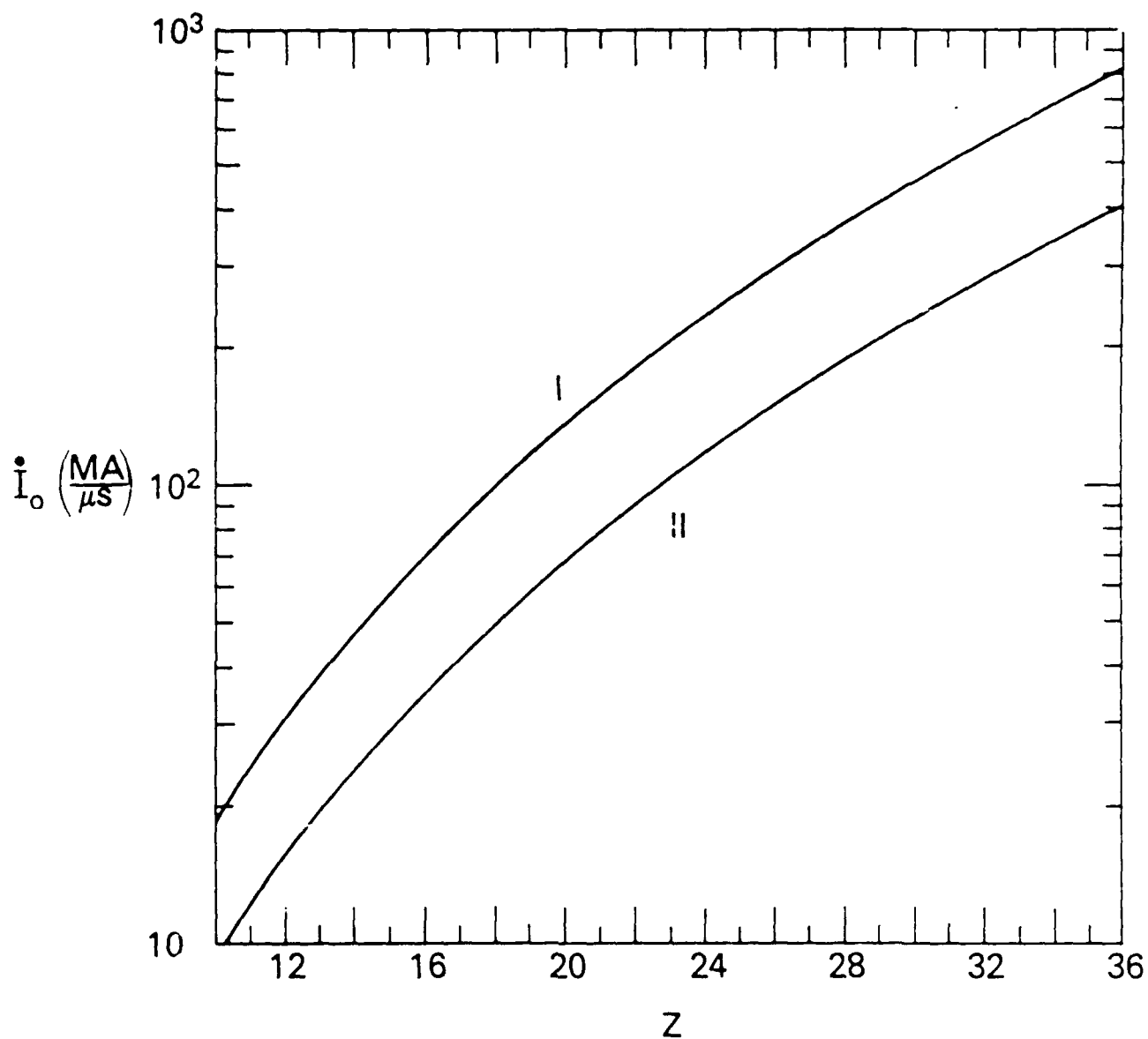


Figure 6. The scaling of the I-dot of the array implosion as a function of atomic number is shown for the two cases (I and II) described in the text.

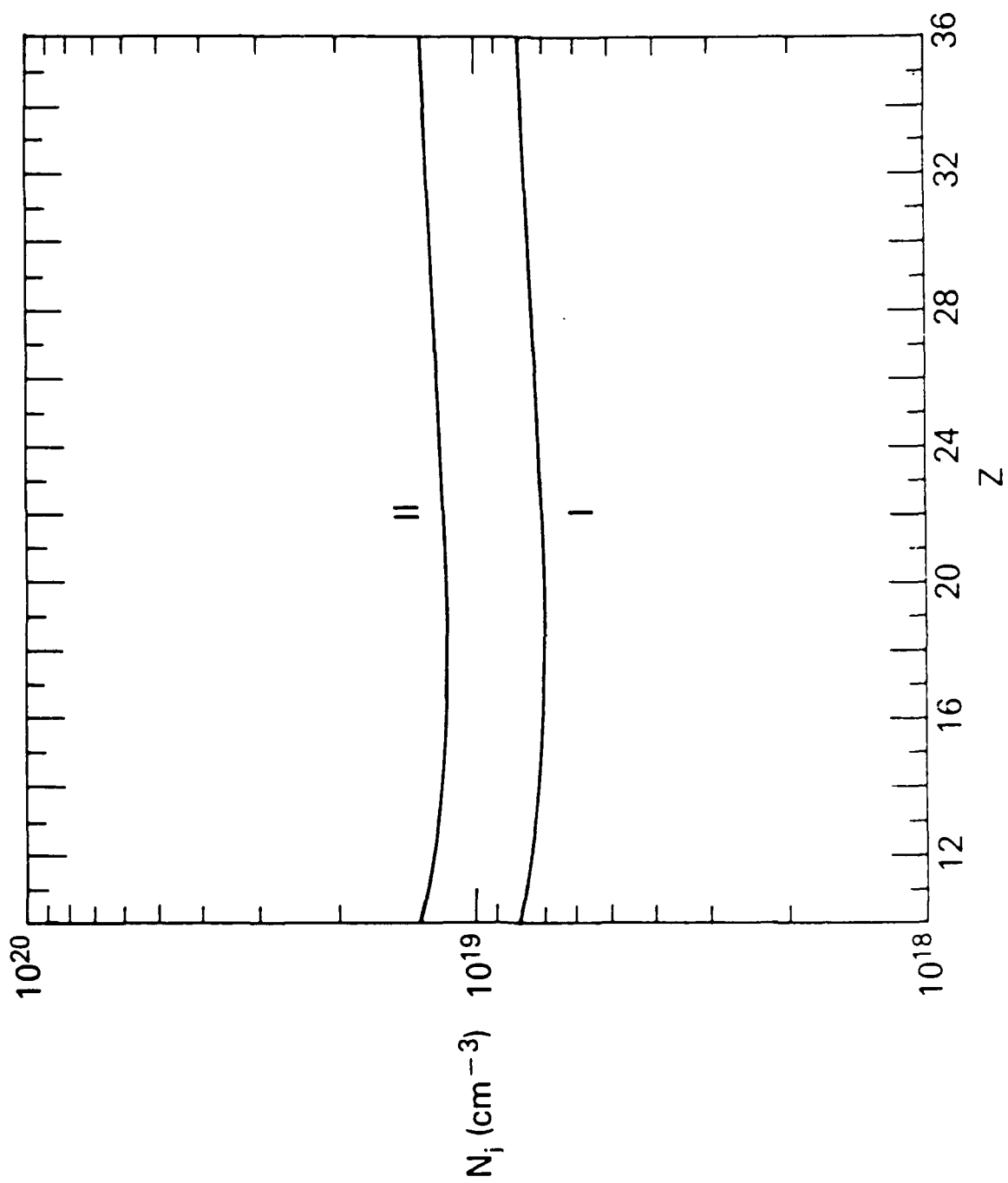


Figure 7. The final ion density that is achieved in the two array implosions, I and II, is shown as a function of atomic number.

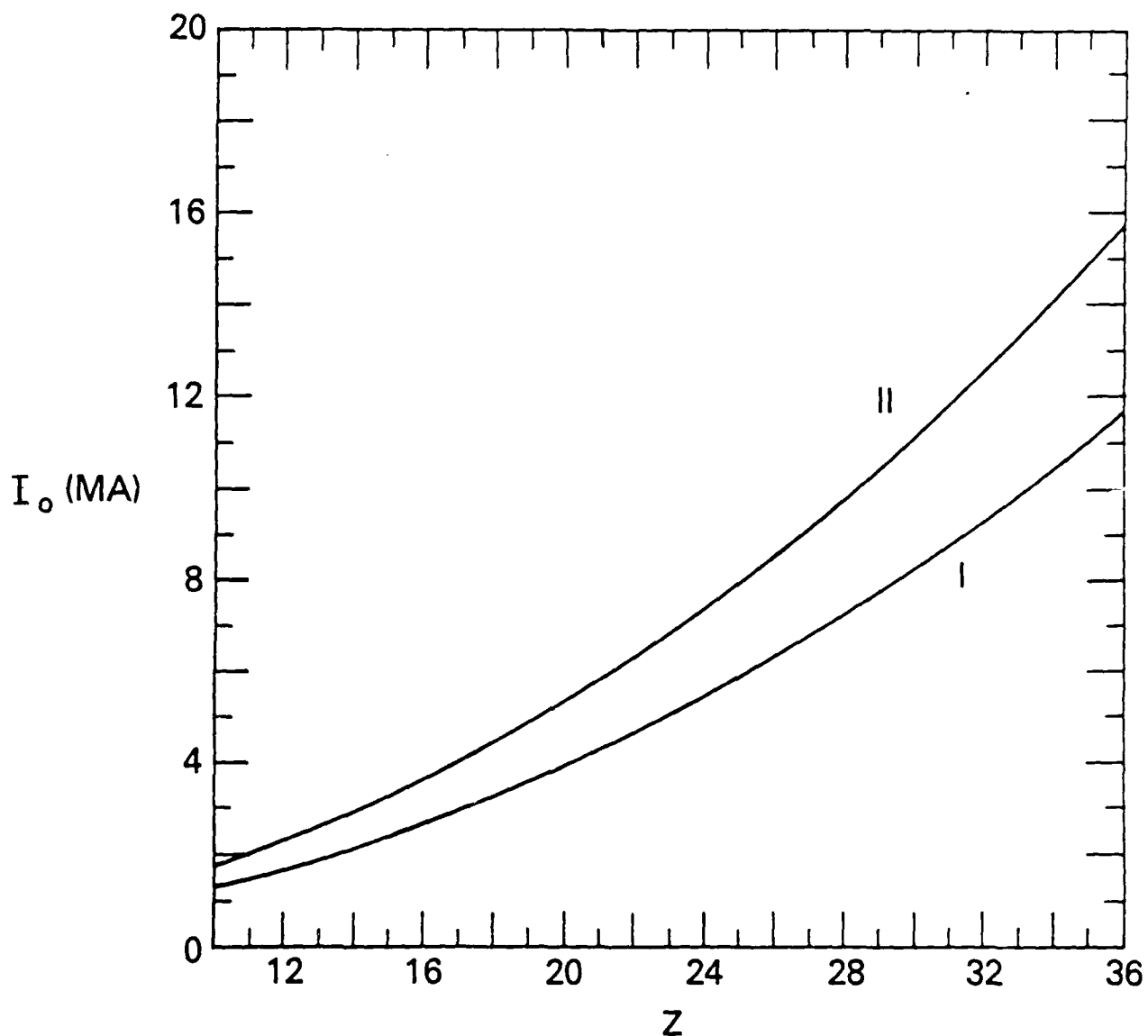


Figure 8. The peak current that is needed at the end of the array implosion in the two cases, I and II, to sustain a linear growth in current is shown as a function of atomic number.

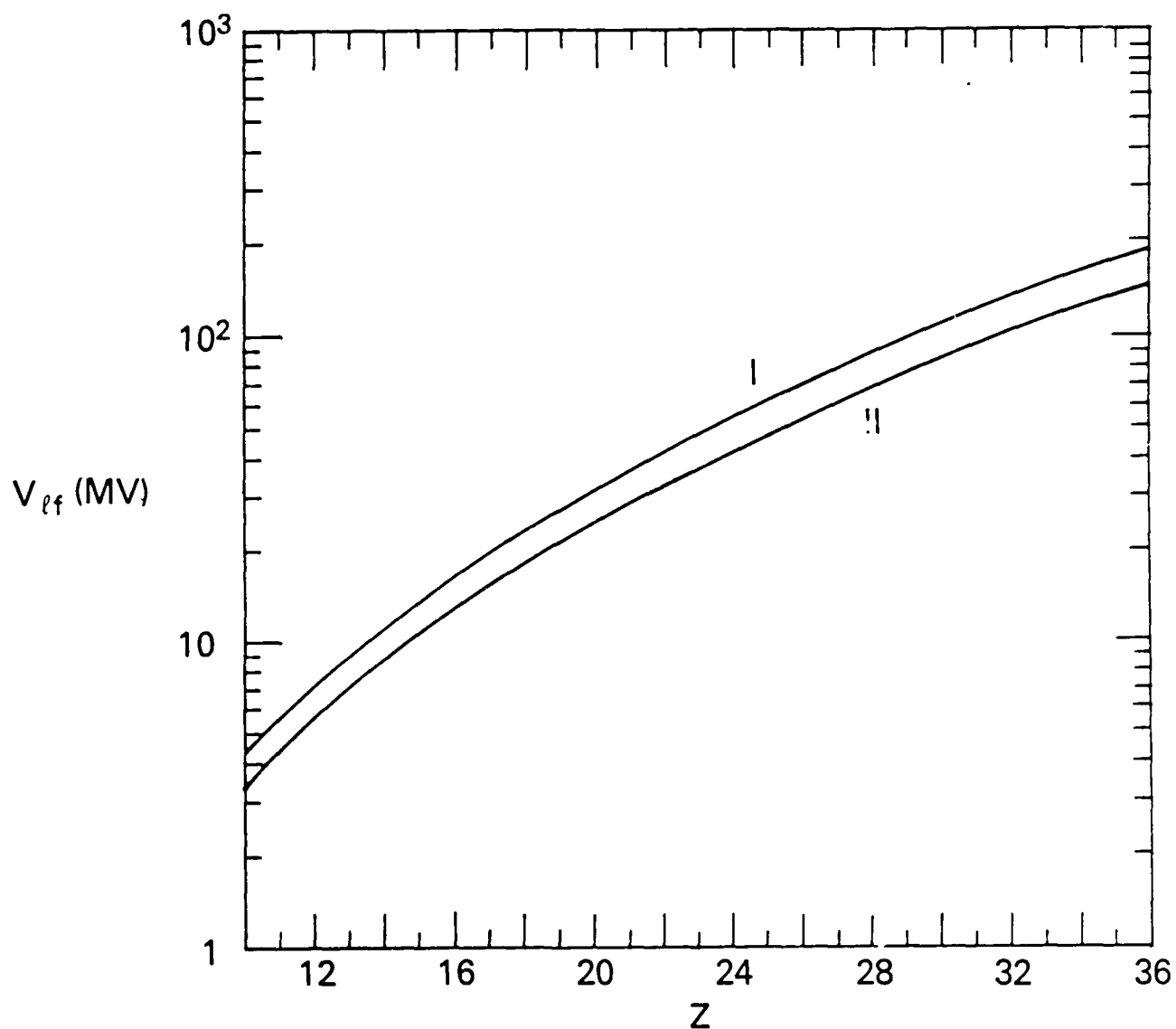


Figure 9. The final voltage that is impressed across the z-pinch in order to drive the peak current through the plasma in the two cases described in the text is shown as a function of atomic number.

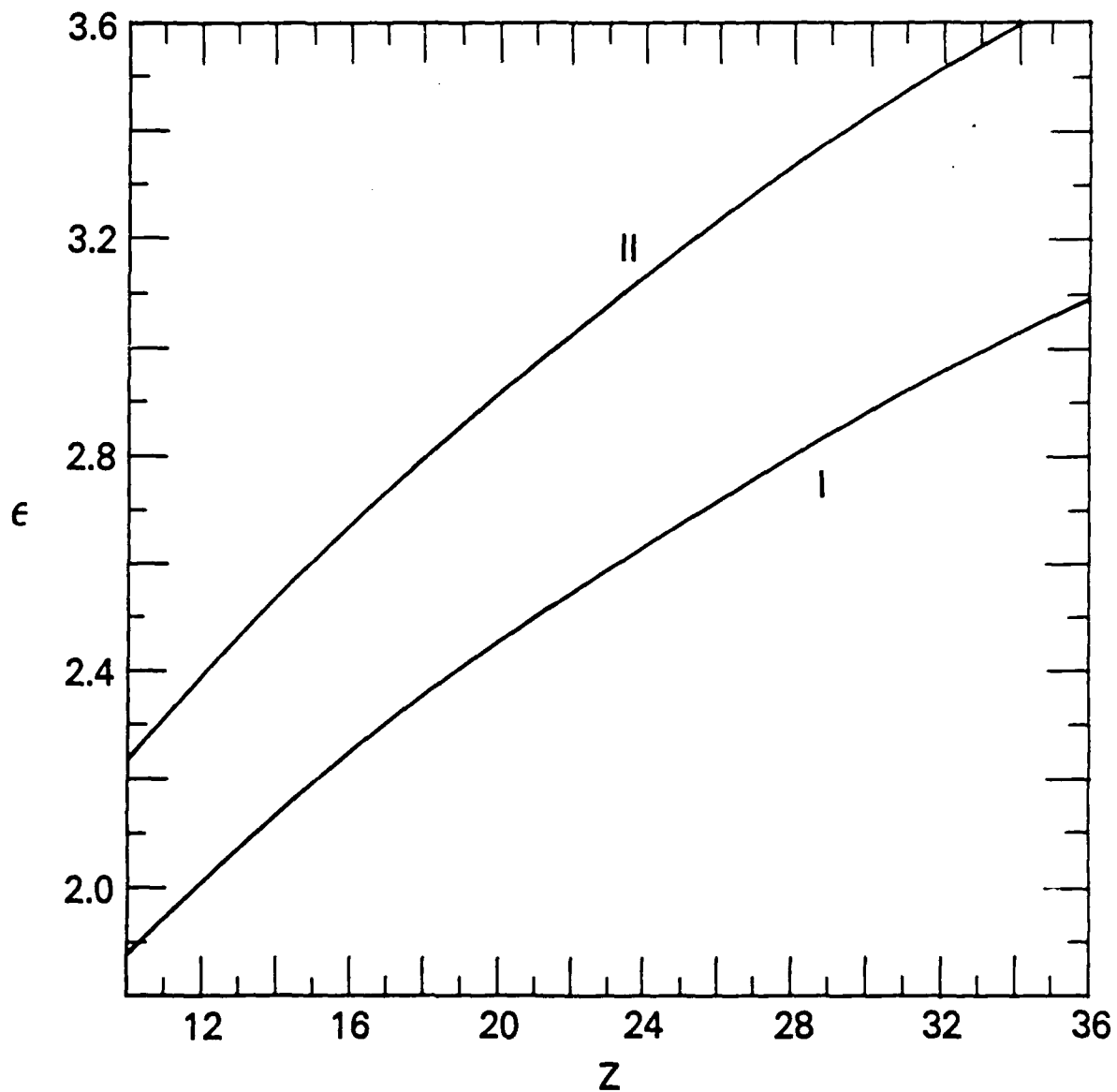


Figure 10. The thermalization efficiency that is needed to achieve force balance at the final radius of the implosion is shown as function of atomic number, for the two cases, I and II.

DISTRIBUTION LIST

Assistant to the Secretary of Defense Atomic Energy Washington, D.C. 20301 Attn: Executive Assistant	1 copy
Director Defense Nuclear Agency Washington, D.C. 20305 Attn: DDST TITL RAEV STVI	1 copy 4 copies 1 copy 1 copy
Commander Field Command Defense Nuclear Agency Kirtland AFB, New Mexico 87115 Attn: FCPR	1 copy
Director Joint Strat TGT Planning Staff Offutt AFB Omaha, Nebraska 68113 Attn: JLKS	1 copy
Undersecretary of Defense for RSCH and ENGRG Department of Defense Washington, D.C. 20301 Attn: Strategic and Space Systems (OS)	1 copy
Deputy Chief of Staff for RSCH DEV and ACQ Department of the Army Washington, D.C. 20301 Attn: DAMA-CSS-N	1 copy
Commander Harry Diamond Laboratories Department of the Army 2800 Powder Mill Road Adelphi, Maryland 20783 Attn: DELHD-N-NP DELHD-TA-L (Tech. Lib.)	1 copy each
U.S. Army Missile Command Redstone Scientific Information Center Attn: DRSMI-RPRD(Documents) Redstone Arsenal, Alabama 35809	3 copies
Commander U.S. Army Nuclear and Chemical Agency 7500 Backlick Road Building 2073 Springfield, Virginia 22150 Attn: Library	1 copy

Commander Naval Intelligence Support Center 4301 Suitland Road, Bldg. 5 Washington, D.C. 20390 Attn: NISC-45	1 copy
Commander Naval Weapons Center China Lake, California 93555 Attn: Code 233 (Tech. Lib.)	1 copy
Officer in Charge White Oak Laboratory Naval Surface Weapons Center Silver Spring, Maryland 20910 Attn: Code R40 Code F31	1 copy each
Weapons Laboratory Kirtland AFB, New Mexico 87117-6008 Attn: Dr. William Baker SUL CA	1 copy each
Deputy Chief of Staff Research, Development and Accounting Department of the Air Force Washington, D.C. 20330 Attn: AFRDQSM	1 copy
Commander U.S. Army Test and Evaluation Command Aberdeen Proving Ground, Maryland 21005 Attn: DRSTE-EL	1 copy
Auburn University Department of Physics Attn: Dr. J. Perez Auburn, Al 36849	1 copy
AVCO Research and Systems Group 201 Lowell Street Wilminton, Massachusetts 01887 Attn: Library A830	1 copy
BDM Corporation 7915 Jones Branch Drive McLean, Virginia 22101 Attn: Corporate Library	1 copy
Berkeley Research Associates Post Office Box 983 Berkeley, California 94701 Attn: Dr. Joseph Workman	1 copy

Berkeley Research Associates Post Office Box 852 5532 Hempstead Way Springfield, Virginia 22151 Attn: Dr. Joseph Orens	1 copy each
Boeing Company Post Office Box 3707 Seattle, Washington 98134 Attn: Aerospace Library	1 Copy
General Electric Company - Tempo Center for Advanced Studies 816 State Street Post Office Drawer QQ Santa Barbara, California 93102 Attn: DASIAC	1 Copy
Institute for Defense Analyses 1801 N. Beauregard Street Alexandria, Virginia 22311 Attn: Classified Library	1 copy
IRT Corporation Post Office Box 81087 San Diego, California 92138 Attn: R. Mertz	1 copy
JAYCOR 1608 Spring Hill Road Vienna, Virginia 22180 Attn: R. Sullivan	1 copy
JAYCOR 11011 Forreyane Road Post Office Box 85154 San Diego, California 92138 Attn: E. Wenaas F. Felbar	1 copy
KAMAN Sciences Corporation Post Office Box 7463 Colorado Springs, Colorado 80933 Attn: Library	1 copy each
Lawrence Livermore National Laboratory University of California Post Office Box 808 Livermore, California 94550 Attn: DOC CDN for 94550 DOC DCN for L-47 L. Wouters DOC CDN for Tech. Infor. Dept. Lib.	1 copy each

Lockheed Missiles and Space Company, Inc. Post Office Box 504 Sunnyvale, California 94086 Attn: S. Taimlty J.D. Weisner	1 copy each
Maxwell Laboratory, Inc. 9244 Balboa Avenue San Diego, California 92123 Attn: A. Kolb M. Montgomery K. Ware	1 copy ea.
McDonnell Douglas Corporation 5301 Bolsa Avenue Huntington Beach, California 92647 Attn: S. Schneider	1 copy
Mission Research Corporation Post Office Drawer 719 Santa Barbara, California 93102 Attn: C. Longmire	1 copy each
Mission Research Corporation-San Diego 5434 Ruffin Road San Diego, California 92123 Attn: Victor J. Van Lint	1 copy
Northrop Corporation Northrop Research & Technology Center 1 Research Park Palos Verdes Peninsula, California 90274	1 copy
Physics International Company 2700 Merced Street San Leandro, California 94577 Attn: C. Deeney T. Nash	1 copy each
R and D Associates Post Office Box 9695 Marina Del Rey, California 90291 Attn: Library	1 copy each
Sandia National Laboratories Post Office Box 5800 Albuquerque, New Mexico 87115 Attn: Doc Con For 3141 D. McDaniel P. VanDevender K. Matzen, Code 4247	1 copy each
Science Applications, Inc. 10260 Campus Point Drive Mail Stop 47 San Diego, California 92121 Attn: R. Beyster	1 copy

Science Research Laboratory
150 Ballena Blvd., Suite 100
Alameda, California 94501
Attn: M. Krishnan

Spectra Technol, Inc.,
2755 Northup Way
Bellevue, Washington 98004
Attn: Alan Hoffman

1 copy

Spire Corporation
Post Office Box D
Bedford, Massachusetts 07130
Attn: R. Little

1 copy

S-CUBED
Post Office Box 1620
La Jolla, California 92038
Attn: A. Wilson

1 copy

Director
Strategic Defense Initiative Organization
Pentagon 20301-7100
Attn: T/IS Dr. Dwight Duston

1 copy

Texas Tech University
Post Office Box 5404
North College Station
Lubbock, Texas 79417
Attn: T. Simpson

1 copy

TRW Defense and Space Systems Group
One Space Park
Redondo Beach, California 90278
Attn: Technical Information Center

1 copy

Naval Research Laboratory
Radiation Hydrodynamics Branch
Washington, D.C. 20375
Code 4720 - 50 copies
4700 - 26 copies
2628 - 22 copies